

# Viscoelastic Properties And Curing Of Polyhedral Oligomeric Silsesquioxanes POSS Modified Ethylene-Propylene Hydrogenated Nitrile Rubber EPM/HNBR Composites

Magdalena Lipińska<sup>a</sup>, Mateusz Imiela<sup>a</sup>

Lodz University of Technology,  
Institute of Polymer and Dye Technology  
90-924 Lodz, Poland  
e-mail: magdalena.lipinska@p.lodz.pl

**Abstract**— Viscoelastic properties and curing of ethylene-propylene hydrogenated nitrile rubber EPM/HNBR modified by addition of methacryloisobutyl silsesquioxane (MIB-POSS) and octavinyl silsesquioxane (OV-POSS) were investigated. The melt viscosity, shear storage modulus  $G'$  and  $\tan \delta$  were used for analyzing the rheological behavior of uncured EPM/HNBR composites. It was found that the methacryloisobutyl-POSS decreased the dynamic complex viscosity  $\eta^*$ . The presence of organic isobutyl chains in MIB-POSS improve melting and exerted plasticizing effect on uncured EPM/HNBR composites. The OV-POSS influenced curing of EPM/HNBR composites, it modified kinetic of peroxide curing and significantly enhanced crosslink density of EPM/HNBR composites. The studies confirmed that POSS moieties had strong impact on mechanical properties, thermo-oxidative ageing and solvent resistance of EPM/HNBR composites. Dynamic mechanical investigations have revealed that the EPM/HNBR composites were immiscible, two glass temperatures  $T_g$  were indicated. Atomic force microscopy AFM images showed that the presence of OV-POSS at the interface provides higher compatibility and finer morphology of EPM/HNBR composites.

**Keywords**—cure behaviour, rheological properties, rubber, nanoparticles, POSS

## I. INTRODUCTION

Among polymer nanocomposites the thermoplastics, thermoset or elastomer materials reinforced with nanoparticles attracted significant attention due to their improved mechanical, thermal, electrical and optical properties. Usually lower amount of nanoparticles (less than 5% by weight) is necessary to achieve comparable improvements in properties comparing to traditional macro or micro fillers. For this purpose nano-sized inorganic particles such as: spherical nanoparticles (e.g. silica), two-dimensional, with plate-like morphology particles (e.g. layered silicates), one-dimensional nanofibers (e.g. nanotubes, whiskers) or nanometric cage structures (polyhedral oligomeric silsesquioxanes POSS) are used. Polyhedral oligomeric silsesquioxanes (POSS) are three dimensional cage like molecules with the formula  $(RSiO_{1.5})_n$  (where the  $n = 6, 8, 10$  or higher) having an inorganic silica core surrounded by wide

range of organic groups (R) at the corners of the cage. The most commonly studied POSS structure is octameric POSS ( $R_8Si_8O_{12}$ ) [1-4]. Published research focuses on the application of POSS moieties as nanoscale physical property modifiers [5,6]. The R substituents which can be either hydrogen, inert organic or reactive groups incorporated into polymeric matrices effectively lead to structural and functional modifications of polymers. Various length organic chains may improve solubility and affinity to nonpolar matrices, while one or more reactive functionalities are available for grafting and thus can act as interfacial modifiers for various composite material. POSS cages with one reactive group can be grafted onto the polymer backbone as a side groups. Two reactive groups give possibility of POSS incorporation as comonomeric units in composite synthesis. POSS with more than three reactive groups may act as chemical crosslinks. Grafting of POSS moieties may improve polymer properties, maximum use temperature, oxidation resistance, mechanical properties and reduce flammability. A number of publications show the advantages of POSS application in polyolefins [7-8], polystyrene [9], polyamides [10-11] as well as POSS-crosslinked epoxy systems [12-13]. Some authors [14] suggest that a simple blending of POSS containing non-reactive organic groups instead of grafting them may lead to lower improvement in composite properties due to partial incompatibility of POSS with some polymer matrices. Various POSS have been broad studied as a functional additives able to improve the properties of polydimethylsiloxane such as: thermal degradation behavior and thermo-oxidative stability [15-18]. It was found that base on octavinyl-POSS derivative and hydrosilylation reactions a novel crosslinker for room temperature vulcanized silicon rubber octa[trimethoxysilyl]ethyl-POSS can be prepared [1]. The chemical bounded into silicon rubber network POSS cross-linker enhanced thermal and mechanical properties of RTV silicon rubber comparing to silanes based crosslinkers. Effect was attributed to the increased dimensionality of cross-linking network (three dimensional structure of octa[trimethoxysilyl]ethyl-POSS crosslinker), the plasticization of self-cross-linked POSS cross-linker

and uniform distribution of POSS domains in network. Liu et al. [19] prepared the silicon elastomer composites containing POSS by melt blending method. Authors proved that the temperature of POSS-silicone mixing influenced the morphology of blends and the dispersion of highly crystalline octaisobutyl-POSS in poly(methylvinylsiloxane) due to possibility of POSS melting and recrystallization in different morphology and aggregates shape during cooling. Octaisobutyl-POSS and allylisobutyl-POSS were incorporated into poly(methylvinylsiloxane) chemically crosslinked by peroxide [20]. Opposite to octaisobutyl-POSS molecules, which aggregated extensively, the chemical tethering of allylisobutyl-POSS in polymer backbone avoided the formation of POSS large aggregates and resulted in changes of composites morphology. The authors [20] proved that the morphology of final composites depended on amount of reactive for grafting and polymerization POSS molecules. The crystallization of the octamethyl-POSS and octaisobutyl-POSS molecules in the ethylene-propylene (EP) copolymers were also observed [21]. The oscillatory rheological studies in the molten state indicated that two types of interaction in EP/POSS melts occurred: strong particle-to-particle interactions in POSS crystals and the weak particle-to-matrix interactions between POSS crystals and ethylene-propylene matrix. Many authors observed the benefit of POSS application on the thermal stability of a various polymeric systems [22-24]. Many studies confirmed that for various POSS/rubber containing systems the chemical linking between POSS and polymer matrix played a predominated role in composite properties improvement [2, 25]. In more morphologically complex systems as a segmented polyurethane elastomers or other phase segregated materials e.g. polymers blends the influence of POSS on the existing morphology is complicated and thus not by any means exclusively predictable. The nitrile-butadiene rubber NBR composites with enhanced mechanical properties were obtained by constructing a novel network structures containing octa-(polyethylene glycol)-POSS cages [26]. The effective crosslinks based on the coordination ability of electron-rich groups (-CN and -C-O-C- groups) to interact with metal cations ( $Li^+$ ) which were formed in NBR/LiClO<sub>4</sub>/POSS network strongly increased the 300% modulus and tensile strength of composites. According to some publications POSS with organo-functional groups such as glycidyl [27], epoxycyclohexyl [28], hydroxyl [29] groups can interact with carboxyl groups and provide crosslinked sites for carboxylated nitrile-butadiene rubber XNBR increasing crosslinking density, mechanical properties, glass transition temperature, ageing resistance. In this work we used two various POSS derivative containing methacryl and vinyl groups to prepare elastomer composites based on hydrogenated nitrile HNBR and ethylene-propylene rubber EPM. The possibility of POSS participation in curing reactions via reactive functional groups is expected to give improvement in the properties of EPM/HNBR/POSS composites.

Recently fabrication of two or more elastomer blends is a very advantageous way of developing new materials combining properties of individual constituents. Blending two or more elastomers is carried out in order to improve special properties e.g. chemical and ageing resistance, processing characteristics, mechanical properties. Acrylonitrile-butadiene rubber is most widely used polar rubber which exhibits particularly the excellence resistance to oil and fuel. Ethylene-propylene rubber is less expensive, additionally characterizes good ageing resistance and balanced water and heat stability. The thermodynamic incompatibility between components of rubber blends can lead to poor interfacial adhesion and results in deterioration of final material properties. Several strategies have been reported to improve compatibility of various polymer and elastomers blends, among them, the incorporation of a third polymeric component [30-31], the selective incorporation in one phase the components (accelerators) of curing system [32, 33]. It is well known that hybrid nanoparticles with different surface chemistries show higher efficiency in compatibilizing immiscible polymer blends [34]. In our work we propose a reactive compatibilizing of EPM/HNBR composites by application of nanoparticles such as functionalized POSS able to grafting during peroxide crosslinking, together with nanometric silicas and cationic layered double silicates acting as reinforcing fillers. Herein, the viscoelastic properties, the rheometric curing characteristic of these materials, crosslink density, and mechanical properties are analyzed. The atomic force microscopy AFM and dynamic mechanical measurements DMA were conducted to detect the polymer compatibility within the rubber composites. Additionally the ageing stability and chemical resistance were investigated.

## II. EXPERIMENTAL

### A. Materials

The rubber composites were prepared using: hydrogenated acrylonitrile-butadiene rubber HNBR (Terban 3407, Arlanxco) containing  $34 \pm 1.0$  wt.% acrylonitrile (ISO 24698-1) and <0.9% of residual double bonds after hydrogenation, ethylene-propylene copolymer EPM (Dutral CO 054, Versalis S.p.A.) containing 41 wt.% propylene. Composites were crosslinked with 2.5 phr of (bis(1-methyl-1-phenylethyl) peroxide) DCP (Sigma-Aldrich). Polyhedral oligomeric silsesquioxanes POSS were obtained from Hybrid Plastics: methacryloisobutyl POSS (MA0702, CAS: 307531-94-8) containing one methacryl group and seven isobutyl groups and octavinyl POSS (OL1170). The 3 phr (parts per hundred of rubber) of POSS were used for every rubber composites formulation. As a reinforcing filler were applied: 20 phr of fumed silica Aerosil 380 (Evonik) and 5 phr of montmorillonite Nanomer I.31PS, product of Nanomer Clay, contains according to product data sheet 0.5-5wt% aminopropyl-triethoxysilane and 15-35 wt% octadecylamine.

### B. Preparation of EPM/HNBR composites

Two steps melt compounding method was applied to obtain EPM/HNBR composites. In first step, the composites of HNBR and EPM containing POSS and organic modified montmorillonite OMT were prepared separately using Brabender Measuring Mixer N50. The rubber compounds were processed using 50 rpm (revolution per minute) rotor speed at the initial temperature 60°C. After 5 minutes of rubber mastication POSS was added and mixed for 15 minutes, then organic modified montmorillonite was added and mixed during additional 15 minutes. In the next step both compounded rubbers EPM and HNBR were homogenized together with peroxide curing system and silica in a laboratory two-roll mill (temperature 40°C, friction ratio 1:1.2, dimension of rolls- diameter 200 mm, length 450 mm) during 15 minutes. Additionally, the EPM/HNBR composites containing POSS and silica added during homogenization of both rubbers using a laboratory two-roll mill were prepared. For every EPM/HNBR composite the ratio of pure EPM to pure HNBR was 50:50.

### C. Techniques

The MDR rheometer RPA 3000 MonTech with the lower die of the chamber oscillated sinusoidally at a fixed angle 7% and frequency 1.67 Hz was used to characterize curing of EPM/HNBR composites. Uncured composites behavior was studied according to ASTM D6204 Part A (low strain) and Part B (high strain) standards. The viscoelastic measurements were made based on a frequency sweep in which the frequency was programmed to change in three steps 0.1 Hz, 2.0 Hz, 20Hz under constant strain amplitude 7% and to change in two-steps 0,1 Hz, 1 Hz under constant strain amplitude 100%, the temperature of measurements was 100°C. Before the measurement the conditioning step during 5 minutes at frequency 0.5 Hz and 2.8% strain was carried out. The curing studies were done at 160°C according to ASTM D5289. After curing during 30 min at 160°C additional measurements of two-cycle strain sweep were made in which the strain amplitude was programmed to change in five steps, 1%, 2%, 5%, 10%, 20% under constant frequency 10 Hz and temperature 100°C. The compounded blends were molded and vulcanized using electrically heated hydraulic press under a pressure of 5 MPa at their optimum curing time. Cured sheets were conditioned before testing (24 h maturation at room temperature). The network structure was analyzed according to ASTM D 6814-02 standard. Weighed rubber samples were swollen at room temperature (25°C) in solvent (reagent grade purity toluene) for the time necessary to achieve weight balance of swelled samples (48h). The solvent were replaced with fresh toluene from time to time. After swelling the excess liquid was removed from the surface of the specimens with a soft paper towel and the samples were weighted. In the next step, the specimens were dried at 50°C in a forced-ventilating air oven for 24 h until constant mass. The dried

samples were cooled down to room temperature (25°C) using a desiccator and weighted again.

Stress-strain behavior was characterized using Zwick 1435 tensile machine. The moduli at 100, 200, 300% elongation, tensile strength, and elongation at break were measured at 25°C with crosshead speed of 500 mm/min for testing type 1 dumb-bell specimens prepared according to ISO-37-2005 standard. Five different specimens were tested and the average value for each formulation was reported. Shore A hardness was determined using an automatic Zwick Roell Durometer, on cylindrical samples have an effective thickness of 6 mm according ASTM D-2240 after 15 s of indentation. Dynamic mechanical measurements were carried out in tension mode using DMTA V viscoanalyser (Rheometric Scientific). Measurements of the dynamic moduli were performed over the temperature range (-100 - 100C) with a heating rate of 2°C/min, at the frequency of 1Hz and a strain amplitude of 0.02%.

Micromorphology analysis of the composites was tested by atomic force microscope "Metrology Series 2000" (Molecular Imaging, USA) in tapping mode. Probe for imaging NSC16 (MicroMasch, Estonia), with resonant frequency 170 kHz and constant elasticity 40 N/m, ended with silicone tip, scanned surface of the sample with frequency of 4 Hz. A freeware scanning probe microscopy software WSXM based on MS-Windows was used to measure different plots on a fixed surface point and process the images [35].

Thermal oxidative ageing was performed in Memmert ovens with forced convection at 70±2°C and 50% of humidity during 14 days. The retained percentage values of tensile strength, elongation at break were measured before and after the aging studies. The determination of the effect of liquids on vulcanized rubber were done according to PN-ISO1817 standard. The percentage of mass increase were calculated after 7 days of swelling in various solvents. Pure grade ethanol, chloroform, acetone, and reference liquid of composition containing different ratio of toluene/2,2,4-trimethylpentane were used. Five samples of similar volume were used for every measurement.

## III. RESULTS AND DISCUSSION

### A. Influence of POSS on viscoelastic behavior and curing of EPM/HNBR composites

The dynamic oscillating rheometers, RPA are able to measure dynamic viscosity when a sinusoidal strain is applied to a molded, uncured rubber composites. The viscoelastic nature of tested uncured rubber causes that the complex torque response  $S^*$  is observed to be out-of-phase with the applied strain. The out-of-phase response is quantified by the phase angle  $\delta$ . The elastic torque  $S'$  (in-phase with applied strain) and the viscous torque  $S''$  (90° out-of-phase with the applied strain) can be derived from the complex torque response  $S^*$  and the phase angle  $\delta$  [36]. The storage shear modulus  $G'$  is calculated from the equations:



$$G' = k \cdot \frac{s'}{\text{strain}} \quad (1)$$

the loss shear modulus ( $G''$ ):

$$G'' = k \cdot \frac{s''}{\text{strain}} \quad (2)$$

where  $k$  is constant connected with the geometry of the die cavity.

The complex shear modulus  $G^*$  is equal to:

$$G^* = [(G')^2 + (G'')^2]^{\frac{1}{2}} \quad (3)$$

the complex dynamic viscosity  $\eta^*$  and the real dynamic viscosity  $\eta$  is calculated as follows:

$$\eta^* = \frac{G^*}{\omega}, \eta' = \frac{G'}{\omega} \quad (4)$$

The complex dynamic viscosity  $\eta^*$  measured using oscillating rheometers RPA is analogous to the apparent (uncorrected) viscosity  $\eta_{app}$  measured by the capillary rheometer, while the real dynamic viscosity is analogous to the "corrected" viscosity from capillary rheometer [37-40]. Rubber compounds are non-Newtonian fluids and their behavior usually is characterized by shear thinning, the decrease of viscosity with increasing shear rate. Plotted log-log curves of dynamic complex viscosity  $\eta^*$  against shear rates usually showed linear profiles. As shown in Fig. 1 and Fig. 2 the frequency sweep log-log curves of RPA dynamic complex viscosity for the EPM/HNBR composites show very good linear correlation. Various flow behavior of the uncured EPM/HNBR composites containing POSS moieties is observed. The addition of metacryloisobutyl-POSS changed the dynamic complex viscosity  $\eta^*$  while the octavinyl-POSS had slight effect on viscosity (Fig. 2). The organic isobutyl chains improve melting and solubility of MIB-POSS in elastomer and exert plasticizing effect on uncured EPM/HNBR composite. Moreover, the uncured MIB-POSS-EPM/HNBR composites containing montmorillonite OMT also characterize lower viscosity at 100°C comparing to these modified with octavinyl-POSS. The plasticizing effect of isobutyl-POSS at higher temperature was previously observed by some authors [19]. Different curve slopes were observed for the uncured POSS-EPM/HNBR composites containing nanometric silica.

Usually various reinforcing fillers have different shear thinning profiles but the strong changes in curves slope indicate that the EPM/HNBR composites containing silica should be processing at higher shear rate to achieve the same processability and decrease of viscosity during processing. Additional short timed 20 seconds tests at 100°C under a constant higher strain amplitude (100%) and frequency (1 Hz) were performed to estimate the effect of POSS and fillers aggregate network on the complex viscosity  $\eta^*$  for uncured mixed batches. These static deformations have an effect on observed complex viscosity  $\eta^*$  values. The higher applied strain is commonly needed to help break up gel structure in raw elastomers and break up filler aggregate networks [29].

Fig. 1. Log-log plot of RPA dynamic complex viscosity  $\eta^*$  versus frequency (rad/s) for uncured MIB-POSS-EPM/HNBR composites (temperature 100°C, applied strain 7%), \* POSS added together with peroxide and silica using two-roll mill

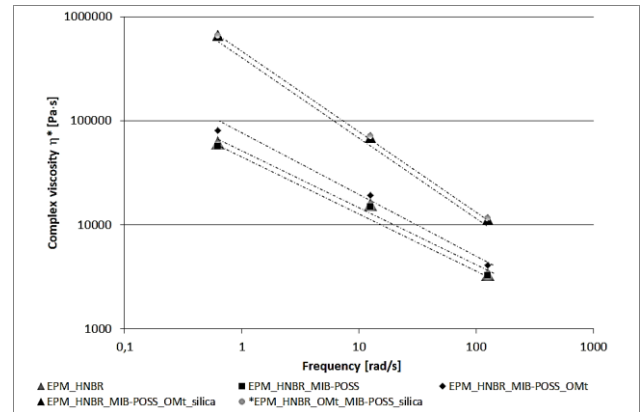
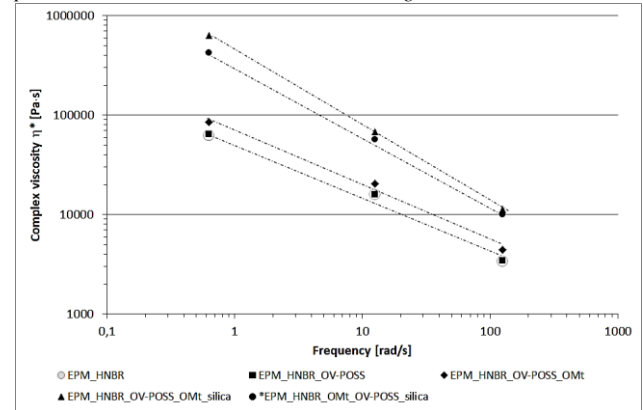
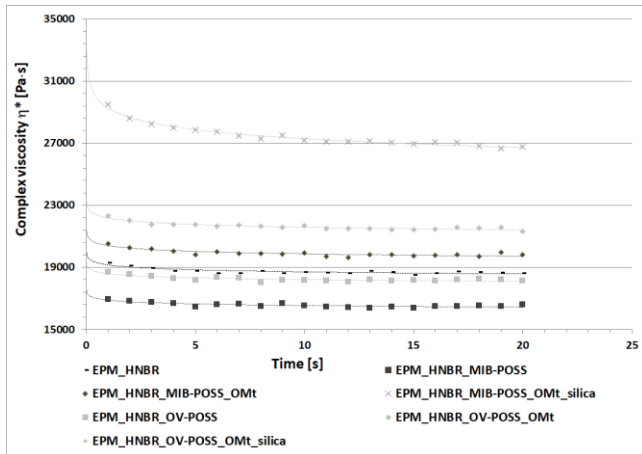


Fig. 2. Log-log plot of RPA dynamic complex viscosity  $\eta^*$  versus frequency (rad/s) for uncured OV-POSS-EPM/HNBR composites (temperature 100°C, applied strain 7%), \* POSS added together with peroxide and silica using two-roll mill.



As is shown at Fig. 3 the montmorillonite filled POSS-EPM/HNBR composites characterize decrease of complex viscosity during first five second of measurement comparing to pure EPM/HNBR composites. Partly, this is because the shape of the particles differ in length/diameter ratio and under high strain the orientation of particles in composite matrix changed. Stronger thixotropic effect, time-dependent shear thinning property are observed for silica filled POSS-EPM/HNBR composites. Silica is stiffening filler, for silica filled composites higher energy and longer time is needed to break up filler aggregates network. It should be also pointed out that the complex viscosity  $\eta^*$  of MIB-POSS-EPM/HNBR composites under these conditions of measurement is much lower than raw EPM/HNBR composites what indicated that addition of POSS influence the processability of composites under high strain condition. The effect is stronger for containing isobutyl groups MIB-POSS.

Fig. 3. Time-dependent shear thinning properties of uncured EPM/HNBR composites (temperature 100°C, strain 100%, frequency 1 Hz), \* POSS added together with peroxide and silica using two-roll mill.



The presence of isobutyl groups influenced on microgel structure of EPM/HNBR composites. The values of storage shear modulus ( $G'$ ) and  $\tan \delta$  at  $100^\circ\text{C}$  for different frequencies are compiled in table 1. Rubber is viscoelastic material in both uncured and cured states. The elasticity of uncured rubber is mainly a result of chain entanglements. It is well known that the elasticity of uncured rubber affects the mixing and processing of rubber. A higher values of storage shear modulus  $G'$  implies a higher elastic response from material at defined frequency, strain and temperature. This higher elastic response resists processing and it affects e.g. how well the rubber incorporates the filler during mixing. Mixed rubber composites with higher  $\tan \delta$  may have stronger die swell, poorer dimensional stability during extrusion process and mold differently from those with lower value of  $\tan \delta$ . Parameters such as  $\tan \delta = G''/G'$  as well as the values of storage shear modulus  $G'$  have been found the sensitive and reliable parameters to estimate differences in processability of uncured rubber composites [37]. Hydrogenated nitrile-butadiene rubber characterizes higher value of storage shear modulus  $G'$  at low frequencies comparing to ethylene-propylene rubber EPM, but the processability of both elastomers and their blend EPM/HNBR is almost similar at higher frequencies. The addition of OV-POSS and organic modified montmorillonite increased the values of storage shear modulus  $G'$  as a result of hydrodynamic effect. The lower values of storage shear modulus  $G'$  and  $\tan \delta$  for MIB-POSS-EPM/HNBR composites at low frequencies, usually used during compression molding and low-shear mixing, indicated that incorporation of second filler, montmorillonite should be easier than for the OV-POSS-EPM/HNBR composites. However the silica filled EPM/HNBR characterized higher values of storage shear modulus which is attributed to strong filler-filler and filler-rubber interactions, the silica filled POSS-EPM/HNBR composites exhibited good processability at higher frequencies.

TABLE I. T VISCOELASTIC PROPERTIES OF UNCURED EPM/HNBR COMPOSITES MODIFIED BY ADDITION OF POSS (TEMPERATURE  $100^\circ\text{C}$ , APPLIED STRAIN 7%).  $G'$  – STORAGE SHEAR

MODULUS, LOSS FACTOR  $\tan \delta = G''/G'$ , \* POSS ADDED TOGETHER WITH PEROXIDE AND SILICA USING TWO-ROLL MILL

Uncured rubber	Frequency Hz	$G'$ kPa	$\tan \delta$
EPM	0.1	13.5	2.3
	2	146.9	0.7
	20	358.4	0.4
HNBR	0.1	38.6	0.9
	2	180.7	0.7
	20	448.1	0.4
EPM/HNBR	0.1	23.64	1.3
	2	162.20	0.7
	20	392.36	0.4
EPM/HNBR/MIB-POSS	0.1	15.9	1.9
	2	148.5	0.8
	20	381.6	0.4
EPM/HNBR/MIB-POSS/OMt	0.1	26.7	1.6
	2	194.4	0.8
	20	477.5	0.4
EPM/HNBR/MIB-POSS/OMt/SiO <sub>2</sub>	0.1	364.7	0.5
	2	779.4	0.5
	20	1326.5	0.4
*EPM/HNBR/OMt/MIB-POSS/SiO <sub>2</sub>	0.1	357.8	0.4
	2	793.4	0.2
	20	1369.6	0.2
EPM/HNBR/OV-POSS	0.1	21.9	1.5
	2	163.2	0.7
	20	399.1	0.4
EPM/HNBR/OV-POSS/OMt	0.1	29.5	1.5
	2	209.8	0.7
	20	516.2	0.4
EPM/HNBR/OV-POSS/OMt/SiO <sub>2</sub>	0.1	351.2	0.5
	2	760.7	0.5
	20	1344.1	0.4
*EPM/HNBR/OMt/OV-POSS/SiO <sub>2</sub>	0.1	212.9	0.7
	2	614.8	0.6
	20	1177.7	0.4

Curing behavior of the EPM/HNBR composites at  $160^\circ\text{C}$  were analyzed. The addition of POSS moieties influenced curing of EPM/HNBR composites what is observed as the changes in the value of the elastic component of the torque  $S'$  for EPM/HNBR composites during curing. In table 2 the values of rheometric curing parameters are compiled. As we supposed MIB-POSS did not affected strong the optimum cure time. This measurement confirmed plasticizing effect of isobutyl groups, the MIB-POSS/EPM/HNBR characterized lower values of minimum torque  $S_L$ . Addition of organic modified montmorillonite to MIB-POSS/EPM/HNBR composites decreased the scorch time and increased the value of maximum torque  $S_H$ . Similar effect was observed after incorporation of silica to EPM/HNBR composites. The higher functionality of POSS (more than one active group) is needed to modify the peroxide curing of the EPM/HNBR composites. The activity of octavinyl-POSS during EPM/HNBR composites curing is confirmed by higher values of CRI indexes calculated according to equation:  $CRI = \frac{100}{\tau_{90} - t_{\Delta 2}}$  (5). Moreover, for all containing OV-POSS-EPM/HNBR composites the

reduction in scorch time  $t_{\Delta 2}$ , optimum cure time  $\tau_{90}$  and strong increase of maximum torque  $S_H$  is observed. The influence of POSS, montmorillonite and silica addition and their reinforcing activity in composites were estimated using Wolff coefficient of activity  $\alpha_F$  [41]. The  $\alpha_F$  parameters for filler systems were calculated according to equations:  $M_{spec} = \frac{\Delta S'_x}{\Delta S'_0} - 1$  (6),  $M_{spec} = \alpha_F \cdot \frac{m_x}{m_p}$  (7), where  $\Delta S'_x$  is the torque increment during curing for EPM/HNBR composites containing x phr of fillers,  $\Delta S'_0$  is the torque increment for non-filled EPM/HNBR composites,  $m_x$  is weight of added fillers,  $m_p$  is weight of elastomers in composites. Higher values of  $\alpha_F$  exhibited EPM/HNBR composites modified with OV-POSS moieties than these modified with MIB-POSS what indicated higher reinforcing activity of octavinyl-POSS. The method of POSS incorporation to silica filled EPM/HNBR composites affected the values of  $\alpha_F$ . Composites containing POSS previously mixed with elastomers, before silica and curing system incorporation characterized higher values of  $\alpha_F$ . Better dispersion of POSS moieties through elastomers matrix is achieved during blending in Brabender mixer than using two-roll mill.

TABLE II. RHEOMETRIC PROPERTIES AND CROSSLINK DENSITY OF EPM/HNBR COMPOSITES MODIFIED BY ADDITION OF METACRYLOISOBUTY-POSS AND OCTAVINY-POSS, \* POSS ADDED TOGETHER WITH PEROXIDE AND SILICA USING TWO-ROLL MILL

	$S'_L$ , dNm	$S'_H$ , dNm	$t_{\Delta 2}$ , min	$\tau_{90}$ , min	CRI, $\text{min}^{-1}$	$\alpha_F$	$v_c \cdot 10^3$ , mole-cm <sup>3</sup>
EPM	0.78	8.16	2.4	16.9	6.9	---	6.1
HNBR	0.82	9.18	1.7	13.0	8.9	---	5.6
EPM/HNBR	0.78	8.10	2.1	14.4	8.2	---	7.5
EPM/HNBR/MIB-POSS	0.63	9.04	2.3	13.5	8.9	4.9	10.3
EPM/HNBR/MIB-POSS/OMt	0.90	10.69	1.7	13.7	8.4	4.2	11.0
EPM/HNBR/MIB-POSS/OMt/SiO <sub>2</sub>	4.16	26.43	0.5	12.5	8.3	7.3	9.1
*EPM/HNBR/OMt/MIB-POSS/SiO <sub>2</sub>	4.07	24.44	0.7	13.1	8.1	6.4	9.8
EPM/HNBR/OV-POSS	0.84	15.65	0.7	10.3	10.4	34.1	25.1
EPM/HNBR/OV-POSS/OMt	1.05	18.68	0.6	10.1	10.5	17.6	25.2
EPM/HNBR/OV-POSS/OMt/SiO <sub>2</sub>	4.12	43.24	0.4	10.5	9.9	15.5	31.0
*EPM/HNBR/OMt/OV-POSS/SiO <sub>2</sub>	3.18	37.23	0.4	10.1	10.4	13.0	23.8

The first derivative gives us information about how whether a function is increasing or decreasing, and by how much it is increasing or decreasing. With respect to the reaction speed which is given by the curves of the first derivative of the elastic torque  $dS'/dt$  versus reaction time (Fig. 4, 5) higher speed of curing have been recorded for EPM/HNBR composites containing OV-POSS. For the MIB-POSS-EPM/HNBR composites the induction time defined as the time taken from rheometric test start to reach the point of minimum torque is longer 73 seconds comparing to 15 seconds induction time for OV-POSS-EPM/HNBR composites, and the local maximum of the first derivative  $dS'/dt$  peak appears at longer time which indicates that the reaction speed is slower.

Fig. 4. The first derivative  $dS'/dt$  versus reaction time for MIB-POSS-EPM/HNBR composites.

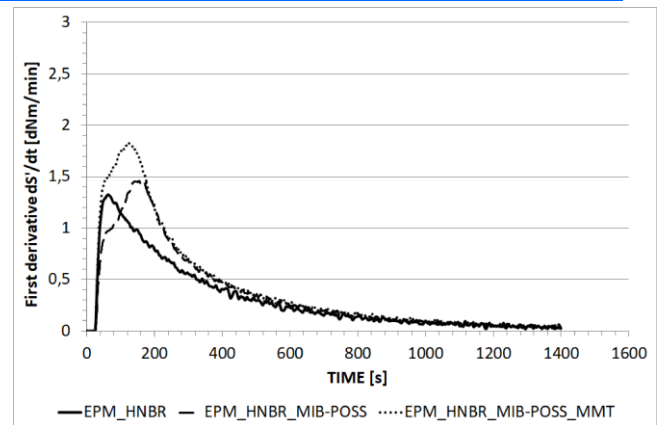
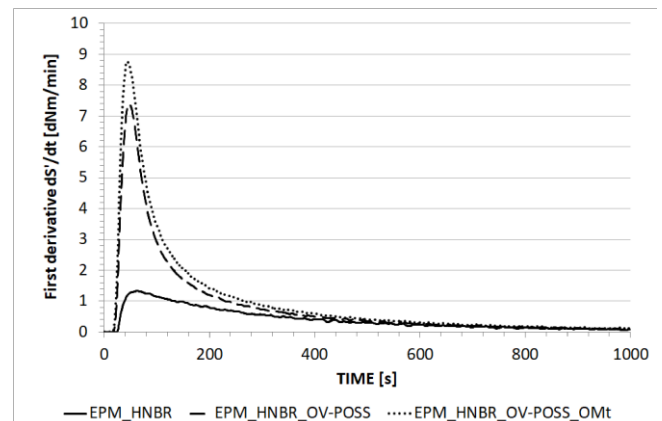


Fig. 5. The first derivative  $dS'/dt$  versus reaction time for OV-POSS-EPM/HNBR composites.



The volume fraction  $V_r$  of rubber in the swollen gel was calculated according to equation:

$$V_r = \frac{(D-FH)/\rho_r}{\frac{D-FH}{\rho_r} + A_0/\rho_s} \quad (8)$$

where H is initial weight of rubber samples, D is constant weight of deswollen specimen, F is weight fraction of insoluble additives such as fillers,  $A_0$  is weight of the absorbed solvent ( $A_0$  – immediate weight after removing from solvent minus initial weight of rubber sample H),  $\rho_r$  is rubber density,  $\rho_s$  is density of the solvent. The classical Flory-Rehner [42] equation at swelling equilibrium condition is given by:

$$-[\ln(1 - V_r) + V_r + \chi V_r^2] = \frac{\rho_r}{M_c} V_s \left( V_r^{\frac{1}{3}} - \frac{2V_r}{f} \right) \quad (9)$$

where f is the cross-linking functionality. Swollen network can be described by phantom network model, which is given by:

$$-[\ln(1 - V_r) + V_r + \chi V_r^2] = \frac{\rho_r}{M_c} V_s \left( 1 - \frac{2}{f} \right) V_r^{\frac{1}{3}} \quad (10)$$

According to the model expressed by above equation the crosslink density  $v_c$  can be calculated from:

$$v_c = \frac{1}{2M_c} = - \frac{\ln(1-V_r) + V_r + \chi V_r^2}{V_s \rho_r \left( V_r^{\frac{1}{3}} - \frac{V_r}{2} \right)} \quad (11)$$

where  $V_r$  is the volume fraction of the polymer in the swollen samples,  $\chi$  is the Flory-Huggins polymer solvent interaction parameter,  $M_c$  is the molecular



weight between cross-links, and  $V_s$  is the molar volume of the solvent. The Huggins parameters ( $\chi$ ) for HNBR-toluene, EPM-toluene and HNBR/EPM-toluene systems are given by the following equations:

$$\chi = 0.501 + 0.273 V_r \text{ (HNBR) (12) [43],}$$

$$\chi = 0.425 + 0.34 V_r \text{ (EPM) (13) [44],}$$

$$\chi = 0.436 + 0.323 V_r \text{ (EPM/HNBR 50:50) (14) [44].}$$

Calculated values of crosslink density are given in table 2. Crosslinking of saturated elastomers has many disadvantages among them long vulcanization time and weak mechanical properties of cured elastomer. Usually to prevent long vulcanization time and improve processing coagents of peroxide crosslinking containing reactive multifunctional vinyl monomers are added. Application of diacrylates and methacrylates as coagents is well known [45]. Both applied POSS increased crosslink density  $v_T$  of EPM/HNBR composites. The application of MIB-POSS together with organic modified montmorillonite led to stronger increase of crosslink density. Layered minerals in combination of unsaturated compounds can act as coagents for crosslinking of HNBR rubber forming additional ionic crosslinks [43]. Probably this effect occurred for EPM/HNBR composites containing MIB-POSS in presence of montmorillonite. In this case additional studies are needed to understand the kinetic mechanism of curing and nature of formed crosslinks. As we supposed OV-POSS significantly enhanced crosslink density of EPM/HNBR composites as a result of participation in network structure. Addition of OV-POSS, together with dicumyl peroxide and silica using two-roll mill instead of mixing it using Brabender mixer caused lower crosslink density of EPM/HNBR composites. Applied higher shear during composite mixing caused more homogenous dispersion of OV-POSS moieties in EPM/HNBR and improved crosslink density of final material.

#### B. Static and dynamic behavior of EPM/HNBR composites.

Reinforcement of composites by active fillers is well-known phenomenon. The addition of fillers has a strong influence on the static and dynamic behavior of composites. The primary particle size and surface area determine interphase filler-polymer contact area. The structure formed by particles of filler, the morphology of filler and its irregularity can restrict motion of elastomer chain under strain and influenced glass transition  $T_g$  and dynamic properties of composites. As a reinforcing fillers nanometric silica Aerosil 380 and organic modified montmorillonite were used. The effect of POSS modification and fillers addition on the mechanical properties of EPM/HNBR composites in static stress-strain measurements were analyzed and the results are summarized in table 3. From the values presented in table 3 can be clearly observed that OV-POSS modification has strong impact on the mechanical properties of EPM/HNBR composites increasing tensile strength TS of vulcanizates. Decrease of elongation at break and

increase of modulus at 100% and 200% elongation observed for samples modified by OV-POSS resulting from the crosslink density increase and incorporation of POSS particles in composite network structure. The higher values of elongation at break  $E_B$  are reported for EPM/HNBR composites modified by MIB-POSS. MIB-POSS improved the tensile strength and modulus of EPM/HNBR composite but did not have strong influence on the mobility of the macromolecules chains during deformation. The incorporation of small quantities of MIB-POSS together with montmorillonite did not caused remarkable increase in tensile strength, observed modulus and strain amplification resulting from the fact that the montmorillonite is the rigid phase causing hydrodynamic effect and occlusion of rubber. Furthermore, it was found that both POSS and montmorillonite increased hardness of EPM/HNBR composites. As it was expected the modification of composites by incorporation of reinforcing nanometric silica led to significant improvement in mechanical strength of composites.

TABLE III. MECHANICAL PROPERTIES OF CURED EPM/HNBR COMPOSITES.  $SE_{100}$ ,  $SE_{200}$  – MODULUS AT 100% AND 200% ELONGATION, TS – TENSILE STRENGTH,  $E_B$  – ELONGATION AT BREAK, H – HARDNESS IN SHORE A SCALE, \* POSS WAS ADDED DURING MIXING OF PREVIOUSLY PREPARED EPM/HNBR/OMT COMPOSITE WITH DICUMYL PEROXIDE AND SILICA USING TWO-ROLL MILL

	$SE_{100}$ , MPa	$SE_{200}$ , MPa	TS, MPa	$E_B$ , %	H, Shore A
EPM	0.69	0.89	1.8	1042	39.4
HNBR	0.86	1.07	8.7	1279	41.7
<b>EPM/HNBR</b>	<b>0.71</b>	<b>0.92</b>	<b>5.4</b>	<b>1220</b>	<b>38.1</b>
EPM/HNBR/ MIB-POSS	0.67	0.95	6.8	1264	39.9
EPM/HNBR/ MIB-POSS/OMt	0.95	1.24	6.3	1142	45.9
EPM/HNBR/ MIB-POSS/OMt/SiO <sub>2</sub>	2.33	3.16	17.4	1139	64.9
*EPM/HNBR/ OMt/MIB-POSS/ SiO <sub>2</sub>	2.17	2.78	14.9	1171	66.4
EPM/HNBR/ OV-POSS	1.11	2.00	7.5	432	49.8
EPM/HNBR/ OV-POSS/OMt	1.52	2.96	9.2	465	57.6
EPM/HNBR/ OV-POSS/OMt/SiO <sub>2</sub>	4.24	7.60	13.9	366	76.2
*EPM/HNBR/ OMt/OV-POSS/ SiO <sub>2</sub>	3.15	5.11	12.7	460	70.9

A dynamic-mechanical analysis was performed to confirm the influence of POSS moieties on glass transition temperatures of EPM/HNBR composites. Presence of two separated glass transition temperatures indicated by two separated loss factor  $\tan \delta$  peaks confirmed that EPM/HNBR were immiscible and two phases existed (table 4). For the unmodified EPM/HNBR composite the first transition observed at -62.3°C was referring to ethylene-propylene EPM phase, second present at -24.5 to nitrile rubber HNBR phase. The different impact of the both POSS on the composites glass transition temperatures was observed. The incorporation of MIB-POSS did not influenced strongly glass transition temperatures of EPM/HNBR composites. The location of each peaks did not show considerable change to neat components. OV-POSS shifted both glass transition temperature towards higher temperatures confirming restricted mobility of the rubber chains due to higher functionality of POSS-crosslinked rubber network. The

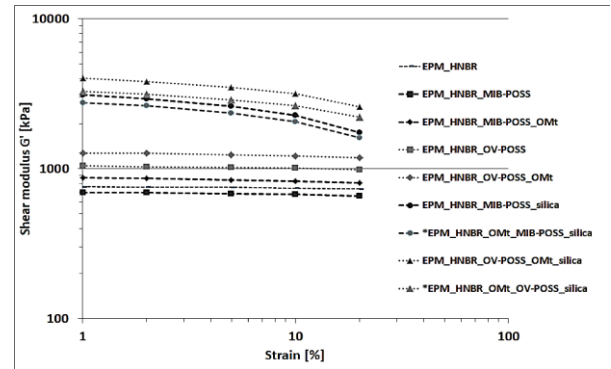
changes in glass transition temperatures of composites after addition of montmorillonite and silica to the POSS modified EPM/HNBR was probably due to differently immobilized elastomer phase on the filler particles surface.

TABLE IV. GLASS TRANSITION TEMPERATURE  $T_g$  OF CURED EPM/HNBR COMPOSITES.

	$T_g$ from $\tan \delta_2$ , °C	$T_g$ from $\tan \delta_3$ , °C
EPM	-60.2	---
HNBR	---	-24.1
<b>EPM/HNBR</b>	<b>-62.3</b>	<b>-24.5</b>
EPM/HNBR/MIB-POSS	-60.9	-24.1
EPM/HNBR/MIB-POSS/OMt/SiO <sub>2</sub>	-61.0	-22.5
EPM/HNBR/OV-POSS	-55.2	-23.5
EPM/HNBR/OV-POSS/OMt/SiO <sub>2</sub>	-58.0	-22.7

A study of the frequency dynamic properties for cured EPM/HNBR composites was carried out using RPA rheometer, the temperature was 100°C and frequency 10Hz (Fig. 6). The effect of increasing strain amplitude on the storage shear modulus  $G'$  was analyzed. Similar to the model of Payne [46] we saw for the OV-POSS-EPM/HNBR composites and for OV-POSS-EPM/HNBR composites containing organic modified montmorillonite OMt the strain independent part of the modulus referring to polymer network and contribution from hydrodynamic effects. Polymer network contribution depends on crosslink density of elastomer and structure and functionality of the network thus the values of the shear modulus  $G'$  for the OV-POSS-EPM/HNBR composites were higher comparing to  $G'$  values of unmodified EPM/HNBR composites. Small effect of the filler-polymer structure was observed for OV-POSS-EPM/HNBR composites containing OMt. Higher values of modulus were attributed to higher amount of occluded rubber which prevented deformation and increased the effective filler content. Different polymer network structure for MIB-POSS-EPM/HNBR composites in which grafted and occluded by rubber chains MIB-POSS moieties were acting as a area able to reversible deformation caused decrease of storage shear modulus  $G'$  comparing to unmodified EPM/HNBR composites. Montmorillonite as a rigid phase which cannot be deformed caused increase of modulus resulting from the hydrodynamic effect for MIB-POSS/OMt/EPM/HNBR composites. The decrease of shear modulus for silica filled EPM/HNBR composites were attributed to the breakdown of the silica-aggregate network. The method of composite preparation influenced the formation of filler network. The silica filled EPM/HNBR composites containing POSS added during higher shear mixing (in Brabender mixer) characterized stronger stress softening effect at small amplitudes and higher Payne effect.

Fig. 6. Strain amplitude dependence of storage shear modulus  $G'$  for cured EPM/HNBR composites (temperature 100°C, frequency 10 Hz).



### C. Determination of the effect of liquids and thermo-oxidative ageing of EPM/HNBR composites

The effect of thermo-oxidative ageing was estimated using  $I_T$  coefficient calculated according to the equation:  $I_T = \frac{(TS \cdot E_B)_{after\ ageing}}{(TS \cdot E_B)_{before\ ageing}}$  (15),

where TS is tensile strength and  $E_B$  is elongation at break, and the values of  $\Delta$  coefficients describing decrease or increase of the values such as: tensile strength TS, elongation of break  $E_B$  and crosslink density  $v_c$  after ageing,  $\Delta$  coefficients were defined as:

$$\Delta A = \frac{(A_{after\ ageing} - A_{before\ ageing})}{A_{before\ ageing}} * 100\% \quad (16)$$

where A were adequately tensile strength, elongation of break and crosslink density before and after ageing. The values of  $I_T$  and  $\Delta A$  coefficients are summarized in table 5.

The  $I_A$  values about 1 indicated minimal changes in mechanical properties after ageing. Based on the obtained  $I_T$  values, which correspond to the thermo-oxidative ageing stability addition of POSS to EPM/HNBR composites provided increase of ageing stability. This behavior may be explained by the increased crosslink density and higher compatibility of EPM and HNBR in composites. The exposure of MIB-POSS-EPM/HNBR and OV-POSS-EPM/HNBR composites containing organic modified montmorillonite to higher temperature resulted in higher stiffness and a loss of elasticity which is reflected by reduced elongation at break  $E_B$ . The values of  $I_T$  coefficient for OMt filled composites decreased. The influence of thermo-oxidative ageing on the crosslink density of montmorillonite filled MIB-POSS-EPM/HNBR and OV-POSS-EPM/HNBR composites was observed. Effect of crosslink density decrease was lower for montmorillonite filled OV-POSS-EPM/HNBR composites. Under elevated temperature conditions the breaking of the polymer chains can occur. Because the OV-POSS characterizes higher functionality and can act as multifunctional network crosslinks balanced the deleterious effect of thermo-oxidative ageing on crosslink density. The silica filled OV-POSS-



EPM/HNBR composites characterized excellent thermo-oxidative ageing stability.

TABLE V. INFLUENCE OF THERMO-OXIDATIVE AGEING ON THE PROPERTIES OF CURED EPM/HNBR COMPOSITES.  $I_A$  COEFFICIENT AND  $\Delta T_S$ ,  $\Delta E_B$ ,  $\Delta V_c$  % COEFFICIENTS DESCRIBING DECREASE OR INCREASE OF THE VALUES AFTER AGEING

	$I_A$	$\Delta T_S$ %	$\Delta E_B$ %	$\Delta V_c$ * $10^5$ %
EPM	1.1	-11	+32	+10
HNBR	0.7	-23	-13	-7
EPM/HNBR	1.5	+33	+13	+13
EPM/HNBR/ MIB-POSS	0.9	-9	-1	-3
EPM/HNBR/ MIB-POSS/OMt	0.4	-35	-39	-16
EPM/HNBR/ MIB-POSS/OMt/ SiO <sub>2</sub>	1.0	+6	-7	+3
EPM/HNBR/ OV-POSS	1.1	+4	+5	-0.5
EPM/HNBR/ OV-POSS/OMt	0.6	-23	-20	-1
EPM/HNBR/ OV-POSS/OMt/SiO <sub>2</sub>	1.0	+7	-6	+4

In order to assess the solvent resistance of cured EPM/HNBR composites the percentage of mass increase  $\Delta m_{100}$  in various liquids was calculated using following equation:  $\Delta m_{100} = \frac{m_i - m_0}{m_0} * 100$  (17), where  $m_0$  is mass of the sample before swelling in liquid,  $m_i$  is sample mass weighted immediately after removing from solvent.

TABLE VI. PERCENTAGE OF MASS INCREASE AFTER SWELLING (7 DAYS) IN VARIOUS LIQUIDS FOR EPM/HNBR COMPOSITES. A - COMPOSITION OF LIQUID: TOLUENE 100% VOL., B - COMPOSITION OF LIQUID: TOLUENE 50% VOL., 2,2,4-TRIMETHYLPENTANE 50% VOL., THF - TETRAHYDROFURAN

	A %	B %	ethanol %	acetone %	THF %	chloroform %
EPM	309	389	0.4	5.9	204	798
HNBR	235	89	8.6	154.1	516	1096
EPM/HNBR	311	252	4.0	57.8	317	786
EPM/HNBR/ MIB-POSS	273	208	3.1	57.4	296	784
EPM/HNBR/ MIB-POSS/OMt	129	207	4.9	59.3	204	732
EPM/HNBR/ MIB-POSS/OMt/SILICA	204	165	6.9	49.7	247	626
EPM/HNBR/ OV-POSS	170	123	4.3	50.9	203	459
EPM/HNBR/ OV-POSS/OMt	160	118	4.6	47.4	184	443
EPM/HNBR/ OV-POSS/OMt/SILICA	113	89	5.2	33.7	117	291

Many organic solvents causes swelling of cured rubber. The extent of swelling depends on compatibility of rubber and solvent and the similarity of their solubility parameters According to rule "like dissolves like" polar solvents will tend to dissolve more polar polymer (HNBR) and non-polar solvents to dissolve non-polar polymer (EPM). For the same rubber the amount of solvent trapped in swollen material, the degree of swelling and the mass and volume expansion of crosslinked network on swelling depend on degree of crosslinking. Additionally the migration of solvent throughout the material, the time of diffusing substance passing a section of surface and volume of the material can be restricted by the presence of solid particles (barrier effect). Blending of ethylene-propylene copolymers with nitrile rubber is simple way of improving the oil resistance. The

EPM/HNBR composites have lower hydrocarbons swelling comparing to EPM rubber. Addition of organic modified montmorillonite and nano-sized silica to EPM/HNBR composites led to further decrease of mass expansion after hydrocarbons swelling. Incorporation of both POSS in EPM/HNBR composites structure caused the reduction of swelling in polar solvents comparing to unmodified EPM/HNBR composites. Blending of EPM with HNBR and modification of material by grafting OV-POSS moieties significantly decreased the chloroform and tetrahydrofuran swelling comparing to unmodified EPM/HNBR composites as well as to both pure rubbers.

#### D. AFM morphology of EPM/HNBR composites

Fig. 7-10 displays the tapping mode AFM (TM-AFM) phase images for POSS modified EPM/HNBR composites. The morphology of EPM/HNBR composites can be deduced by using tapping mode because of its different viscoelastic properties. The dark colored phase in phase images show the lower modulus area, lower modulus rubber in the composites (EPM) and the bright area show higher modulus area (HNBR) and the presence of the solid particles for the filled composites. The figures for filled POSS modified EPM/HNBR composites show a good dispersion and distribution of silica particles inside the matrix (Fig. 9,10). Comparing phase images for MIB-POSS modified EPM/HNBR composite (Fig.7) with OV-POSS modified (Fig 8) it was found that the use of OV-POSS results in a finer morphology. Therefore, the presence of OV-POSS at the interface provides higher compatibility. However it should be noted that the composites still showed two glass temperatures. Further investigations and optimization of composition is needed.

FIG. 7 AFM IMAGE OF MIB-POSS MODIFIED EPM/HNBR COMPOSITE

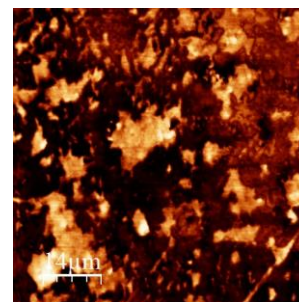


FIG. 8 AFM IMAGE OF OV-POSS MODIFIED EPM/HNBR COMPOSITE

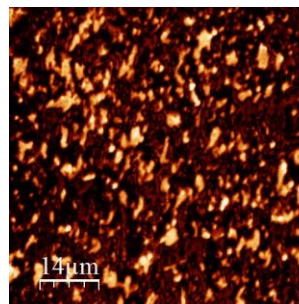


FIG. 9 AFM IMAGE OF MIB-POSS MODIFIED SILICA AND MONTMORILLONITE FILLED EPM/HNBR COMPOSITE

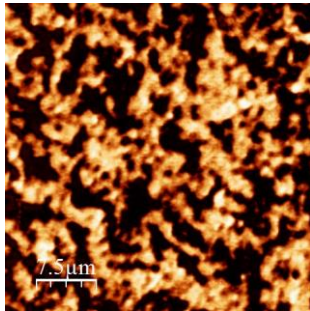
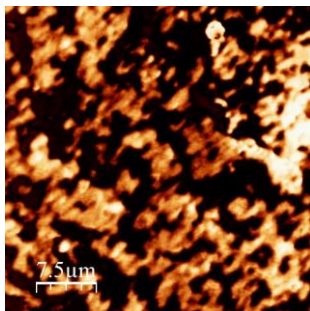


FIG. 10 AFM IMAGE OF MIB-POSS MODIFIED SILICA AND MONTMORILLONITE FILLED EPM/HNBR COMPOSITE



## CONCLUSIONS

In our work various nanocomposites based on ethylene-diene copolymer and hydrogenated butadiene-acrylonitrile rubber EPM/HNBR with improved mechanical properties are reported. The effect of different functionality polyhedral oligometric silsesquioxanes, methacryloisobutyl-POSS and octavinyl-POSS on morphology, rheology and curing characteristics has been investigated. The addition of methacryloisobutyl-POSS decreased the dynamic complex viscosity of uncured EPM/HNBR composites. Organic isobutyl chains present in MIB-POSS influenced the melting behavior. The rheometric characteristics indicated that the optimal curing time for OV-POSS modified EPM/HNBR composites decreased. As we supposed OV-POSS significantly increased the speed of curing and participated in crosslinking reactions. Both POSS led to significant improvement in tensile strength TS of composites. Remarkable enhancement of hardness resulting from higher density of the OV-POSS-EPM/HNBR composites was observed. The AFM analysis showed that nanocomposites based on EPM/HNBR rubber blends exhibited different morphology. Higher compatibility and finer morphology was observed for OV-POSS modified EPM/HNBR composites. The presence of two different immiscible phases was confirmed by appearance of two glass temperatures  $T_g$ . Compared to pure EPM/HNBR composites incorporation of OV-POSS and MIB-POSS into polymer network structure together resulted in higher thermo-oxidative ageing stability and higher solvent resistance.

## REFERENCES

- [1] D.Chen, S.Yi, P.Fang, Y. Zhong, Ch.Huang, X.Wu Synthesis and characterization of novel room temperature vulcanized (RTV) silicone rubbers using octa[(trimethoxysilyl)ethyl-POSS as cross-linker. *React Funct Polym*, 71, pp.502-511, 2011 doi:10.1016/j.reactfunctpolym.2010.12.010
- [2] JP. Lewicki, K. Pielichowski, M. Jancia, E. Hebda, Degradative and morphological characterization of POSS modified nanohybrid polyurethane elastomers . *Polym Degrad Stab*, 104, pp. 50-56, 2014 dx.doi.org/10.1016/j.polyimdegradstab.2014.03.025
- [3] L. Liu, M. Tian, W. Zhang, L. Zhang , JE. Mark . Crystallization and morphology study of polyhedral oligomeric silsesquioxane (POSS)/polysiloxane elastomer composites prepared by melt blending. *Polym*, 48, pp. 3201-3212, 2007 doi:10.1016/j.polymer.2007.03.067
- [4] D. Ambrożewicz, B.Marciniak, T. Jesionowski, New POSS/magnesium silicate nano-hybrids obtained by chemical or mechanical methods. *Chem Eng J*, 210, pp. 229-236, 2012 doi.org/10.1016/j.cej.2012.08.075
- [5] KN. Raftopoulos, K. Pielichowski, Segmental dynamics in hybrid polymer/POSS nanomaterials. *Prog Polym Sci*, 52, pp.136-187, 2016, dx.doi.org/10.1016/j.progpolymsci.2015.01.003
- [6] W. Zhang, G. Camino, R. Yang Polymer/polyhedral oligomeric silsesquioxane (POSS) nanocomposites: An overview of fire retardance. *Prog Polym Sci*, 67, pp. 77-125, 2017 dx.doi.org/10.1016/j.progpolymsci.2016.09.11
- [7] R. Misra, BX Fu, SE. Morgan Surface Energetics, Dispersion, and Nanotribomechanical Behavior of POSS/PP hybrid nanocomposites. *J Polym Sci Part B Polym Phys*, 45, pp. 2441-2455, 2007 doi:10.1002/polb.21261
- [8] JH. Chen, YD. Chiou , Crystallization Behavior and Morphological Development of Isotactic Polypropylene Blended with Nanostructured Polyhedral Oligomeric Silsesquioxane Molecules. *J Polym Sci Part B Polym Phys*, 44, pp.2122-2134, 2006 doi:10.1002/polb.20878
- [9] NT Dintcheva, E. Morici, R.Arrigo, FP. La Mantia, V. Malatesta, JJ. Schwab. Structure-properties relationships of polyhedraloligomeric silsesquioxane (POSS) filled PS nanocomposites. *eXPRESS Polym Lett*, 6(7), pp. 561-571, 2012 doi:10.3144/expresspolymlett.com
- [10] YL. Liu, HCh. Lee. Preparation and Properties of Polyhedral Oligosilsequioxane Tethered Aromatic Polyamide Nanocomposites through Michael Addition between Maleimide-Containing Polyamides and an Amino-Functionalized Polyhedral Oligosilsequioxane. *J Polym Sci Part A Polym Chem*, 44, pp. 4632-4643, 2006 doi:10.1002/pola.21562
- [11] A. Ullah, J. Alongi, S. Russo Recent findings in (Ti)POSS-based polymer systems. *Polym Bull*, 67, pp. 1169-1183, 2011 doi:10.1007/s00289-011-0445-8
- [12] J. Boček , L. Matějka, V. Mentlík, P. Trnka, M. Šlouf Electrical and thermomechanical properties of

epoxy-POSS nanocomposites. *Eur Polym J* 2011;47:861-872 doi:10.1016/j.eurpolymj.2011.02.023

[13] W. Hao, J. Hu, L. Chen, J. Zhang, L. Xing, W. Yang Isoconversional analysis of non-isothermal curing process of epoxy resin/epoxide polyhedral oligomeric silsesquioxane composites. *Polym Test*, 30, pp. 349-355, 2011 doi:10.1016/j.polymertesting.2011.02.005

[14] S. Zheng, F.J. Feher, J. Xiao, RZ Jin In: Polymer nanocomposites, symposium proceeding series. Materials Research Society, p. 734E, 2002

[15] Y. Liu, Y. Shi, D. Zhang, J. Li, G. Huang Preparation and thermal degradation behavior of room temperature vulcanized silicone rubber-g-polyhedral oligomeric silsesquioxanes. *Polym*, 54, pp. 6140-6149, 2013 dx.doi.org/10.1016/j.polymer.2013.08.041

[16] H. Sirin, M. Kodali, B. Karagac, G. Ozkoc Effect of octamaleic acid-POSS used as the adhesion enhancer on the properties of silicone rubber/silica nanocomposites. *Composites part B*, 98, pp. 370-381, 2016 dx.doi.org/10.1016/j.compositesb.2016.05.024

[17] Y. Zhang, Y. Mao, D. Chen, W. Wu, S. Yi, S. Mo, Ch. Huang Synthesis and characterization of addition-type silicone rubbers (ASR) using a novel cross linking agent PH prepared by vinyl-POSS and PMHS. *Polym Deg Stab* 98, pp. 916-925, 2013 dx.doi.org/10.1016/j.polymdegradstab.2013.01.009

[18] D. Chen, Y. Liu, Ch. Huang Synergistic effect between POSS and fumed silica on thermal stabilities and mechanical properties of room temperature vulcanized (RTV) silicone rubbers, *Polym Deg Stab*, 97, pp. 308-315, 2012

[19] L. Liu, M. Tian, W. Zhang, L. Zhang, J.E. Mark Crystallization and morphology study of polyhedral oligomeric silsesquioxane(POSS)/polysiloxane elastomer composites prepared by melt blending. *Polym*, 48, pp. 3201-3212, 2007 doi:10.1016/j.polymer.2007.03.067

[20] Y. Meng, Z. Wei, L. Liu, L. Liu, Z. Liqun, T. Nishi, K. Ito, Significantly improving the thermal stability and dispersion morphology of polyhedral oligomeric silsesquioxane/polysiloxane composites by in-situ grafting reaction. *Polym*, 54, pp. 3055-3064, 2013 dx.doi.org/10.1016/j.polymer.2013.03.061

[21] B.X. Fu, M.Y. Gelfer, B.S. Hsiao, S. Phillips, B. Viers, R. Blanski, P. Ruth Physical gelation in ethylene-propylene copolymer melts induced by polyhedral oligomeric silsesquioxane (POSS) molecules. *Polym*, 44, pp. 1499-1506, 2003 doi:10.1016/S0032-3861(03)00018-1

[22] H. Xu, S-W. Kuo, J.S. Lee, F.Ch. Chang Preparation, Thermal Properties, and  $T_g$  Increase Mechanism of Inorganic/Organic Hybrid Polymers Based on Polyhedral Oligomeric Silsesquioxanes. *Macromol*, 35, pp. 8788-8793, 2002 doi:10.1021/ma0202843

[23] J.Ch. Huang, Ch.B. He, Y. Xiao, K.Y. Mya, J. Dai, Y. Ping Siow Polyimide/POSS nanocomposites: interfacial interaction, thermal properties and

mechanical properties. *Polym*, 44, pp. 4491-4499, 2003 doi:10.1016/S0032-3861(03)00434-8

[24] Y. Ni, S. Zheng, K. Nie Morphology and thermal properties of inorganic-organic hybrids involving epoxy resin and polyhedral oligomeric silsesquioxanes. *Polym*, 45, pp. 5557-5568, 2002 doi:10.1016/j.polymer.2004.06.008

[25] D. Dasgupta, M. Srividhya, A. Sarkar, M. Dubey, D. Wrobel, A. Saxena. Rubber nanocomposites with polyhedral oligomeric silsesquioxanes (POSS) as the filler. In *Progress in Rubber Nanocomposites*, A volume in Woodhead Publishing Series in Composites Science and Engineering. Elsevier Ltd, 2017, p.231-247 doi:org/10.1016/B978-0-08-100409-8.00007-3

[26] S. Yang, H. Fan, Y. Jiao, Z. Cai, P. Zhang, Y. Li Improvement in mechanical properties of NBR/LiClO<sub>4</sub>/POSS nanocomposites by constructing a novel network structure. *Composites Sci Tech*, 138, pp.161-168, 2017 dx.doi.org/10.1016/j.compscitech.2016.12.003

[27] R. Konnola, R. Nair, K. Joseph Cross-linking of carboxyl-terminated nitrile rubber with polyhedral oligomeric silsesquioxane, cure kinetics. *J Therm Anal Calorim.*, 123, pp. 1479-1489, 2016 doi: 10.1007/s10973-015-5019-9

[28] Q. Liu, W. Ren, Y. Zhang, Y. Zhang A Study on the Curing Kinetics of Epoxycyclohexyl Polyhedral Oligomeric Silsesquioxanes and Hydrogenated Carboxylated Nitrile Rubber by Dynamic Differential Scanning Calorimetry, *J Appl Polym Sci*, 123, pp.3128-3136, 2012 doi:10.1002/app.34954

[29] S. Sahoo, A.K. Bhowmick Polyhedral oligomeric silsesquioxane (POSS) nanoparticles as new crosslinking agent for functionalized rubber. *Rubb Chem Tech*, 80(5), pp. 826-837, 2007

[30] X. Zhao, K. Niu, Y. Xu, Z. Peng, L. Jia, D. Hui, L. Zhang, Morphology and Performance of NR/NBR/ENR ternary rubber composites. *Composites Part B*, 107, pp. 106-112, 2016 dx.doi.org/10.1016/j.compositesb.2016.09.073

[31] J.J. Huang, H. Keskkula, DR Paul Elastomer particle morphology in ternary blends of maleated and non-maleated ethylene-based elastomers with polyamides: Role of elastomer phase miscibility. *Polym*, 47, pp. 624-638, 2006 doi:10.1016/j.polymer.2005.11.087

[32] M.A. Mansilla, A.J. Marzocca About the cure kinetics in natural rubber/styrene butadiene rubber blends at 433 K. *Physica B*, 407, pp. 3271-3273, 2012 doi:10.1016/j.physb.2011.12.084

[33] S. Goyanes, C.C. Lopez, G.H. Rubiolo, F. Quasso, A.J. Marzocca Thermal properties in cured natural rubber/styrene butadiene rubber blends. *Eur Polym J*, 44, pp. 1525-1534, 2008 doi:10.1016/j.eurpolymj.2008.02.016

[34] G. Chen, P. Li, Y. Huang, M. Kong, Y. Lv, Q. Yang, G. Li Hybrid nanoparticles with different surface chemistries show higher efficiency in compatibilizing immiscible polymer blends. *Composites Sci Tech*, 105,



- pp. 37-43, 2014  
dx.doi.org/10.1016/j.compscitech.2014.09.013
- [35] I. Horcas, R. Fernandez, JM. Gomez-Rodriguez, J. Colchero, J. Gomez-Herrero, AM. Baro WSXM: A software for scanning probe microscopy and a tool for nanotechnology. *Rev Sci Instrum*, 78:013705, 2007  
dx.doi.org/10.1063/1.2432410
- [36] SL. Agrawal, S. Chakraborty, S. Mandot, S. Dasgupta, S. Bandyopadhyay, R. Mukhopadhyay, AS. Deuri Mathematical Correlation of Polydispersity using Gel Permeation Chromatography and Rubber Process Analyzer for Raw Rubbers. *J Elastomers Plastics*, 38, pp. 31-40, 2006 doi:10.1177/0095244306054684
- [37] JS. Dick Compound Processing Characteristics and Testing In: Dick JS, editor. *Rubber Technology Compounding and Testing for Performance*. Munich: Hanser Publishers, p.17-43, 2001
- [38] T. Gao, R. Xie, L. Zhang, H. Gui, M. Huang Use of Rubber Process Analyzer for Characterizing the Molecular Weight Parameters of Natural Rubber. *Int J Polym Sci*, ID 517260:1-6, 2015  
dx.doi.org/10.1155/2015/517260
- [39] S. Dasgupta, SL. Agrawal, S. Bandyopadhyay, R. Mukhopadhyay, RK. Malkani, SC. Ameta, Improved Polymer-Filler Interaction with an Ecofriendly Processing Aid. Part 1. *Prog Rubber Plast Recycling Tech*, 25(3), pp. 141-164, 2009
- [40] L. Perko, W. Friesenbichler, W. Obendrauf, V. Buchebner, G. Chaloupka, Elongational viscosity of rubber compounds and improving corresponding models. *Adv Prod Eng Manag*, 8(2), pp. 126-133, 2013  
dx.doi.org/10.14743/apem2013.2.160
- [41] S. Wolff, MJ. Wang Filler—Elastomer Interactions. Part IV. The Effect of the Surface Energies of Fillers on Elastomer Reinforcement. *Rubb Chem Tech*, 65(2), pp. 329-342, 1992 doi:10.5254/1.3538615
- [42] PJ. Flory, J. Rehner, Statistical mechanics of cross-linked polymer networks. II Swelling. *J Chem Phys*, 11, pp. 521-526, 1943 doi:10.1063/1.1723792
- [43] M. Maciejewska, M. Zaborski, A. Krzywania-Kaliszewska Mineral oxides and layered minerals in combination with itaconic acid as coagents for peroxide crosslinking of hydrogenated acrylonitrile-butadiene elastomer. *Comptes Rendus Chemie*, 15, pp. 414-423, 2012 doi:10.1016/j.crci.2012.01.001
- [44] M. Lipińska, M. Zaborski, C. Dębek Układy elastomerowe modyfikowane pochodną oksazoliny. *Przemysł Chemiczny*, 89(4), pp. 462-467, 2010
- [45] FR. De Risis, JWM. Noordermeer Effect of methacrylate co-agents on peroxide cured PP/EPDM thermoplastics vulcanizates. *Rubber Chem Tech*, 80, pp. 83-99, 2007 doi.org/10.5254/1.3548170
- [46] AR. Payne The dynamic properties of carbon black-loaded natural rubber vulcanizates. Part I. *J Appl Polym Sci*, 6, pp. 57-63, 1962  
doi:10.1002/app.1962.070061906